IJPSR (2021), Volume 12, Issue 8 **(Research Article)**

INTERNATIONAL JOURNAL OF PHARMACEUTICAL SCIENCES AND RESEARCH

Received on 03 August 2020; received in revised form, 10 October 2020; accepted, 17 May 2021; published 01 August 2021

GREEN SYNTHESIS OF SILVER NANOPARTICLES USING *SAUROPUS ANDROGYNOUS* LEAF EXTRACT WITH POTENTIAL BIOLOGICAL PROPERTIES

Anu P. Abhimannue * and Ashwathi Menon

Department of Biotechnology, St. Mary's College, St. Mary's College Road, Chembukkav, Thrissur - 680020, Kerala, India.

Keywords:

Sauropus androgynous, Silver nanoparticles, Antibacterial, Anti-helminthic, UV-Visible spectroscopy, Scanning Electron Microscopy

Correspondence to Author:
Dr. Anu P. Abhimannue

Assistant Professor,
Department of Biotechnology, St. Mary's College, St. Mary's College Road, Chembukkav, Thrissur - 680020, Kerala, India.

E-mail: anuabhimannue@gmail.com

ABSTRACT: Nanoparticles are being constantly exploited by the scientific community due to their versatile properties and applications. However, the synthesis of metallic nanoparticles achieved through conventional physical and chemical techniques is quite expensive and a labor-intensive process with serious consequences like instability of nanoparticles and toxic byproducts. Hence, green synthesis utilizing biological systems, including plants, bacteria, yeast, fungi, and algae proves to be a cost-effective and eco-friendly alternative. Plant extracts are a rich source of many bioactive compounds like secondary metabolites and often act as reducing and capping agents in the synthesis of nanoparticles. The present work deals with the synthesis of silver nanoparticles using aqueous leaf extract of *Sauropus androgynous*. Prior to the synthesis, phytochemical analysis and antioxidant potential were evaluated. Physical parameters, including silver metal ion concentration and the temperature were optimized for the effective synthesis of silver nanoparticles. The synthesized nanoparticles were characterized *via* UV-Visible spectroscopy, Fourier transform infrared spectroscopy (FTIR), Scanning Electron Microscopy (SEM), and X-ray crystallography (XRD). Finally, silver nanoparticles were evaluated for their antibacterial and anti-helminthic activity. Green synthesis of silver nano particles using *S. androgynous* was optimized at a conc. of 1mM of silver nitrate at a temperature of 70ºC. The characterization of silver nanoparticles revealed a spherical crystallite nature with particle sizes ranging from 16 nm – 55nm. The nanoparticles exhibited antibacterial and anti-helminthic activity too. Hence, the green synthesized silver nanoparticle could be considered as a promising therapeutic choice against infectious pathological conditions.

INTRODUCTION: Nanomaterials, ranging from 1-100 nm in size, have been a focal point for contemporary researchers because of their characteristic physicochemical properties [1]. Nanoparticles has a plethora of application in the field of health care and cosmetics, food and feed, environmental health, mechanics, space industries, energy science and photo-electrochemical field [2, 3, 4].

QUICK RESPONSE CODE

DOI: 10.13040/IJPSR.0975-8232.12(8).4267-74

This article can be accessed online on www.ijpsr.com

DOI link: http://dx.doi.org/10.13040/IJPSR.0975-8232.12(8).4267-74

A promising application of nanomaterials is in the medical field as antibacterial, playing a significant role in controlling infectious diseases with a lower probability of bacterial resistance [5]. The characteristic features of metal-based nanoparticles like small size, shape, and large surface area significantly contribute to their cellular uptake for antibacterial action [6].

The classic physicochemical synthetic techniques pose serious drawbacks, namely low yield and usage of toxic reagents [7]. Chemical synthesis of nanoparticles often utilizes chemical reductants that are hazardous, and a majority of physical methods fall under the top-down scenario, which is not

considered an appropriate method for the synthesis of low dimension nano-sized particles [8]. Hence, nanotechnology emphasizes the green synthesis of nano biomaterials using biological agents like bacteria, fungi, algae, and plant extracts. Among these, plant extracts are the simplest and easiest for large-scale production [9]. The green synthesized nanoparticles are reported to be reliable, sustainable, rapid, low cost, safe for human use, and eco-friendly [10, 11]. The present study focuses on the green synthesis of nanoparticles using leaf extract of *Sauropus androgynous* for evaluation of its potential biological properties.

MATERIALS AND METHODS:

Collection of Materials: Fresh leaves of *Sauropus androgynous* (L.) Merr plant was collected from Thrissur locality of Kerala, India, during the month of November 2018. The plant was identified by Dr. Regi Raphael, Taxonomist, Department of Botany, St. Mary's College, Thrissur, and deposited in the herbarium with an accession number SMC-010. Silver Nitrate, ampicillin, cefepime, and all other reagents used in this study were of analytical reagent grades from Merck India Pvt. Ltd.

Experimental Worms: Adult earthworms (8-10 cm) belonging to species of *Pheretima posthuma* were collected for this study due to its anatomical and physiological resemblance with the intestinal roundworm parasite of human beings [12]. They are also easily available and hence used as a suitable model for the screening of anthelmintic activity. Adult earthworms were collected from the wet soil of the Thrissur district of Kerala. After collection, the samples were washed with saline water to remove soil and undesirable matter.

Extraction of Sauropus and Rogynous Leaves: Fresh leaves of *Sauropus androgynous* collected were washed with deionized water to remove the contaminants and air-dried for 7 days under shade. 5g of powdered, air-dried leaves were heated in 100 ml distilled water in a water bath at 70 ºC for 45 min. After cooling, the aqueous leaf extract was collected through filtration using Whatman filter paper No.1 and was kept in air tight bottle at 4^0C.

Phytochemical Screening and Estimation of Total Phenolic Content: The presence of phytochemicals in the aqueous leaf extract of *Sauropus androgynous* was determined [13]. Total phenolic content in the extract was determined according to the Folin-Ciocalteu method, and the results were expressed as mg/g Gallic acid equivalents [14]. The absorbance measured at 650 nm in Thermo Fisher Scientific UV-Visible spectro-photometer was plotted on Y-axis against concentration of Gallic acid on X-axis. From this calibration curve, the total phenolic content in the extract was calculated.

Anti-oxidant Assay: The anti-oxidant potential of *Sauropus androgynous* leaf extract was evaluated by DPPH free radical scavenging assay [15]. Varying concentrations of the extract were thoroughly mixed with 1 ml of 100 µM of DPPH and incubated at room temperature for 30 minutes in dark. Butylated hydroxyl toluene (BHT) was taken as a positive control. A reaction system consisting of water and DPPH solution, without plant extract, served as the control. Finally, the absorbance was measured spectrophotometrically at 517 nm, and free radical scavenging activity was calculated as, Free radical scavenging activity (%) = [{AC - AT}/AC] ×100, Where AC is the absorbance of the control and AT is the absorbance of the sample. A graph was plotted with the percentage of scavenging activity on the Y-axis and concentration of the sample on X-axis, and the IC_{50} value was calculated from this graph.

Green Synthesis of Silver Nanoparticles (AgNPs): Prior to green synthesis, metal ion concentration and temperature of incubation resulting maximum yield of AgNPs was optimized [16].

Effect of Metal Ion on AgNPs synthesis: To study the effect of silver nitrate on the synthesis of nanoparticles, different concentrations were used. 10 ml of plant extract and 90 ml of varying concentrations of silver nitrate solution were mixed and incubated at 90^0 C in the water bath for 45 min, followed by overnight incubation in the dark at room temperature. The spectrum was recorded in the range 300 nm to 900 nm for the characteristic peak of AgNPs in the Thermo Fisher Scientific UV-Visible spectrophotometer.

Effect of Temperature on AgNPs Synthesis: The reaction mixture containing plant extract and 1 mM silver nitrate were incubated at different temperatures in a water bath for 45 min followed

by overnight incubation in the dark at room temperature, and the spectrum was recorded in the range 300 nm to 900 nm.

Characterization of AgNPs:

FTIR Analysis: Infrared spectrum was analyzed to know the possible functional groups attached to the surface of nanoparticles. The FTIR study was carried out using a Perkin Elmer FTIR spectrophotometer. The nanoparticles were analyzed in the range 4000-400 cm^{-1} at a resolution of 4 cm^{-1} using KBr pellet method.

Scanning Electron Microscopy (SEM) Analysis: The surface morphology and size of nanoparticles were analyzed using TESCAN VEGA3 LMU Scanning electron microscope. The scanning electron micrograph of gold sputter-coated nanoparticles was taken at 30 KV with a working distance of 4.96 mm at a magnification of 30.4 KX.

XRD Analysis: X-Ray Diffraction pattern of nanoparticles was studied on a Bruker AXS D8 Advance X-ray Diffractometer at the step of 0.020º with an operating voltage of 40 KV and a current of 35 mA with Cu Kα radiation (1.5406 Aº) monochromatic filter range of 10-90º. Diffraction intensities were compared with the standard JCPDS files. Average crystalline size of the nanoparticles was calculated using the Debye-Scherer equation:

$$D = \frac{K\lambda}{\beta cos\theta}$$

Where D is the thickness of the nanocrystals, K is constant, λ is the wavelength of X-rays, β is full width at half maximum, and θ is the Bragg angle.

Biological Application of AgNPs:

Antibacterial Activity: To evaluate the antibacterial activity, agar well diffusion method was employed. To the Muller Hinton agar plates swabbed with bacterial cultures (*Escherichia coli, Staphylococcus aureus, Enterobacter cloaca*), 100 µl of varying concentrations of silver nanoparticles was loaded. Ampicillin was used as a positive control against *Escherichia coli, Staphylococcus aureus,* and cefepime against *Enterobacter cloaca*. After holding the plates at room temperature for about 2 hours to allow diffusion of the extracts into the agar, they were incubated for 24 h at 37 ºC and were observed for a zone of inhibition.

Anti-Helminthic Activity: Anti-helminthic activity of AgNPs synthesized from *S. androgynous* was evaluated on *Pheretima posthuma.* Adult earthworms were treated with 20 ml of varying concentrations of AgNPs in petri-plates. Albendazole was kept as the standard. The time taken for paralysis was recorded when there was no visual movement of the worms except when shaken vigorously. The death time was recorded after confirming that the worms neither moved when shaken vigorously nor when dipped in warm water.

Statistical Analysis: All experiments were carried out in triplicate, and the result expressed as average ± standard deviation. Statistical analysis was done by one-way ANOVA and unpaired t-test having a significance level of 95% confidence interval using GraphPad Prism 5™. A P-value <0.05 was considered statistically significant.

RESULTS AND DISCUSSION:

Phytochemical Screening and Estimation of Total Phenolic acid Content: Qualitative analysis of aqueous leaf extract of *S. androgynous* (L) Merr., confirmed the presence of active phytochemicals **Table 1**. The total phenolic content present in the aq. leaf extract was found to be 87.7925 ± 2.008 µg/ml.

TABLE 1: PHYTOCHEMICAL SCREENING OF AQ. EXTRACTS OF *SAUROPUS ANDROGYNOUS* (L) MERR LEAF SAMPLE

Phytochemical	Test Name	Observations	Presence of Phytochemicals
Alkaloids	Wagner's test	Brownish red precipitate was formed	+
Flavanoids	Aq. NaOH test	A yellow solution with NaOH turned colourless with dilute HCl.	+
Terpenoids	Salkowski test	Reddish brown colour was formed at the interface	+
Phenolic compounds	Ferric chloride test	Greenish brown colour was formed	+
Tannins	Ferric chloride test	Greenish brown colour was formed.	+
Saponins	Frothing test/ foam test	Persistence of frothing was not found.	-

(+ indicates presence & - indicates absence of phytochemical)

DPPH Free Radical Scavenging Activity: The results of DPPH free radical scavenging activity exhibited a concentration-dependent action. With an increase in the concentration of plant extract, an increased DPPH free radical scavenging activity was observed. The IC_{50} value was calculated from the graph and was compared with the positive control, BHT **Table 2**. In the present study, it was observed that *Sauropus androgynous* aq. leaf extract had more pronounced anti-oxidant potential when compared with BHT.

TABLE 2: DPPH FREE RADICAL SCAVENGING ACTIVITY

Sample	IC_{50} value (µg/ml)
Butylated Hydroxy Toluene	150.5221 ± 2.913
Sauropus androgynous aq. leaf extract.	26.8433 ± 1.044

IC_{50} values for the test and the control. All experiments were done in triplicate and the result is expressed as average ± standard deviation

Green Synthesis of Silver Nanoparticles:

Effect of Metal Ion Concentration on Synthesis of Silver Nanoparticles: Effect of metal ion concentration on the synthesis of silver nanoparticles was performed using three different concentrations of silver nitrate (1mM, 2.5mM, and 5mM). UV-Vis spectrum revealed a good plasmon band around 420 nm for 1mM concentration of silver ions **Fig. 1**. The peak obtained with a higher concentration of silver ions was observed to be more flattened. The most flattened peak was obtained with 5mM of silver nitrate, the highest conc. taken up for the study. The results revealed that a 1mM concentration of silver nitrate is the most appropriate for the synthesis of silver nanoparticles.

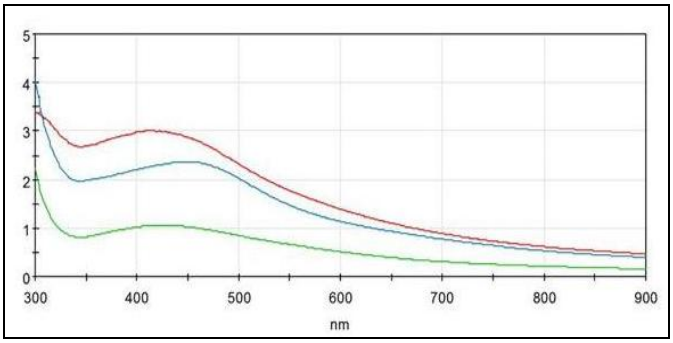

FIG. 1: UV-VIS SPECTRUM SHOWING THE EFFECT OF METAL ION ON SYNTHESIS OF SILVER NANOPARTICLES. --------- representing 1 mM was observed to have characteristic peak whereas ---------- and ---------- spectrum representing 2.5 mM and 5 mM was observed to have flattened peak for the synthesized silver nanoparticles.

Effect of Temperature on Synthesis of Silver Nanoparticles: The effect of different temperature conditions (37 ºC, 50 ºC, and 70 ºC) on the synthesis of silver nanoparticles was evaluated. UV-Vis spectrum was recorded after 24 hrs of incubation, and a good plasmon band around 420 nm was exhibited when the mixture was incubated at 70 ºC **Fig. 2**. At lower temperatures of incubation, no characteristic peak was observed around 420 nm. The color of the reaction mixture was also observed to be more intensified with an increase in the incubation temperature.

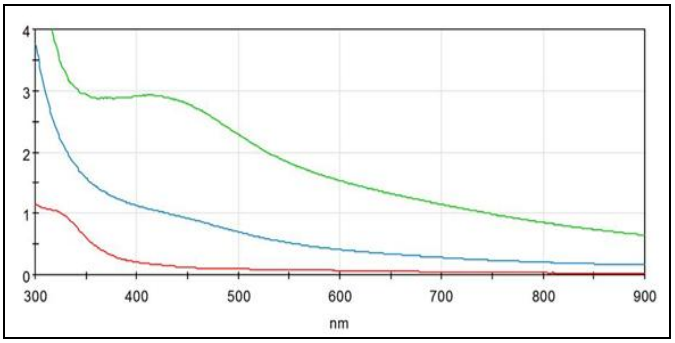

FIG. 2: UV-VIS SPECTRUM SHOWING THE EFFECT OF TEMPERATURE ON SYNTHESIS OF SILVER NANOPARTICLES. --------- and ---------- spectrum representing 37 ºC and 50 ºC was observed to have no peak and ---------- spectrum representing 70 ºC was observed to have characteristic peak for the synthesized silver nanoparticles.

Characterization of Silver Nanoparticles:

FT-IR Spectroscopic Analysis: FT-IR spectroscopic analysis of the aqueous leaf extract of *S. androgynous* and silver nanoparticles was examined to identify the possible biomolecules responsible for capping and stabilization of the nanoparticles **Fig. 3**. The spectrum revealed major peaks in aqueous extract at 3369.09 cm^{-1}, 1620.55 cm^{-1} and minor peak was observed in 2128.02 cm^{-1}, 1281.36 cm^{-1}, 1665 cm^{-1}, and 1053 cm^{-1}. The peaks at 3369.09 cm^{-1} and 1503 cm^{-1} correspond to -O-H- a stretch which can be assigned to H-bonded -O-H stretch and hydroxyl groups. This accounts for the presence of alcohol and phenol groups. This may be from the enzymes and polysaccharides present in the plant extracts.

The peak at 2937cm^{-1} and 1407.73cm^{-1} corresponds to the -O-H- stretching of carboxylic acid. The peak at 2128.02cm^{-1} and 1620.55cm^{-1} corresponds to -C=C stretching of alkene. The peak at -C-N- is due to the presence of aromatic amine. The FTIR spectrum of silver nanoparticles gives a broad peak at 3338.61 cm^{-1} which can be assigned to –O-H stretch of alcohols. A strong IR signal at 1634.19 cm^{-1} corresponds to –C=C stretching vibration.

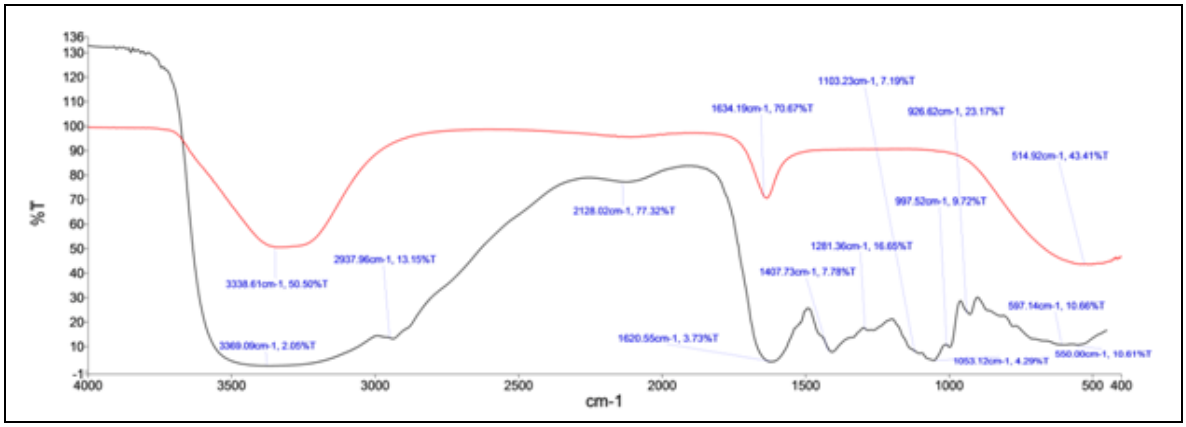

FIG. 3: FTIR SPECTRUM OF SILVER NANOPARTICLES SYNTHESIZED FROM *S. ANDROGYNOUS*

-------- represents the spectrum of silver nanoparticle and ------- represents the spectrum of aqueous leaf extract.

Images taken before and after reduction concludes that all chemical functional groups discussed above may be bound to silver nanoparticles. Reduction of a peak at 2937.96 cm^{-1}, 2128.02 cm^{-1}, 1407.73cm^{-1}, 1281.36 cm^{-1}, 1103.23 cm^{-1}, 997.52cm^{-1}, 926.62cm^{-1}, 597.14cm^{-1} and shifting of peaks at 3369.09 cm^{-1}, 1620.55cm^{-1}, 550.00cm^{-1} indicated the positive role of compounds like flavonoids, phenols, alkaloids, terpenoids, and tannins with –C=C stretching vibrations, -OH groups, amino groups in the process of reduction, capping as well as stabilization for the silver nanoparticles.

Scanning Electron Microscopic (SEM) Analysis: Scanning electron micrograph revealed that the synthesized silver nanoparticles were spherical in shape and the size of the nanoparticles was found to range between 50-55 nm **Fig. 4**.

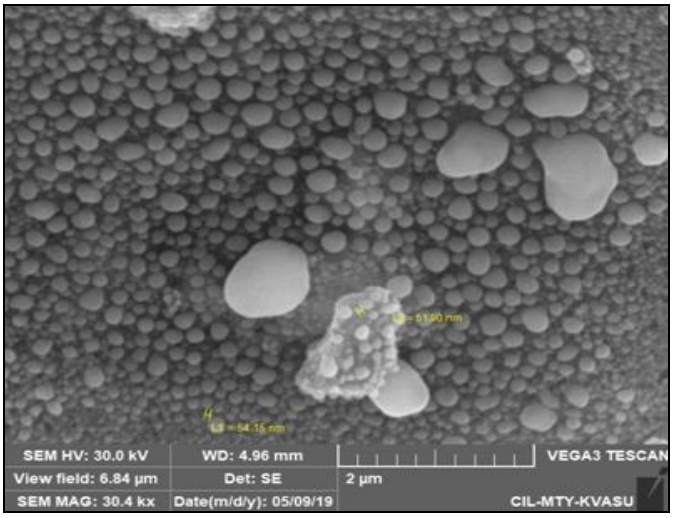

FIG. 4: SEM IMAGE OF SILVER NANOPARTICLE SYNTHESIZED FROM AQUEOUS LEAF EXTRACT OF *S. ANDROGYNOUS* WITH 1MM OF SILVER NITRATE AT 70ºC AND INCUBATED FOR 1 h

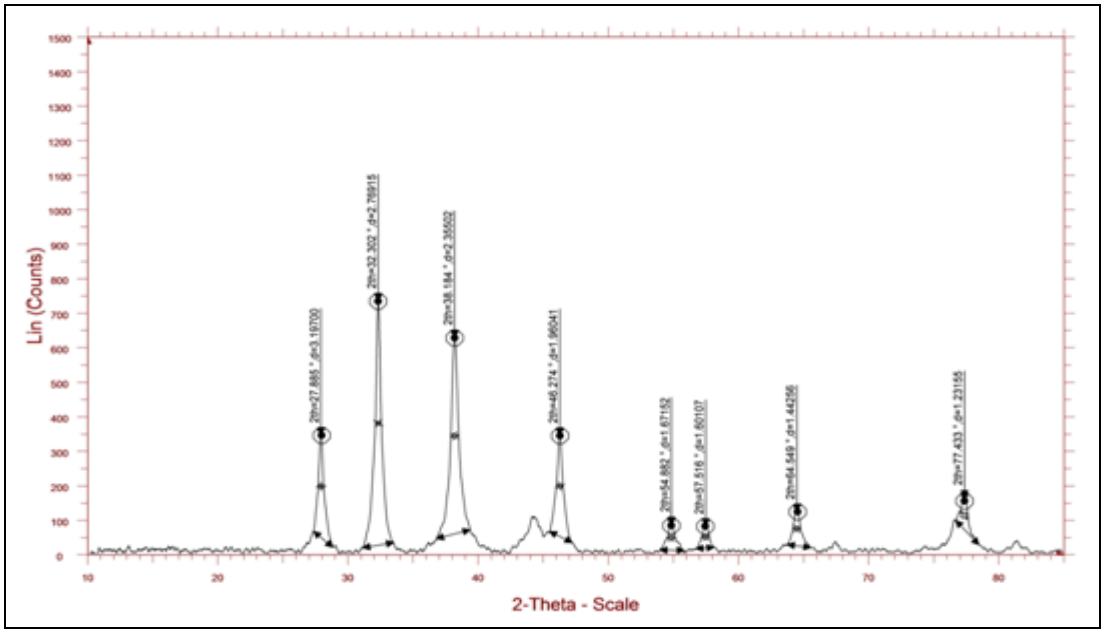

FIG. 5: XRD SPECTRUM OF NANOPARTICLES SYNTHESIZED FROM AQUEOUS EXTRACT OF *S. ANDROGYNOUS*

XRD Analysis: The XRD pattern obtained for silver nanoparticles synthesized using *S. androgynous* gave 4 peaks at 2θ = 38.184º, 46.274º, 64.549º, 77.433º **Fig. 5**. The diffraction peaks observed at 2θ range 30º -80º can be indexed to the (111), (200), (220), (311) planes of fcc silver (JCPDS file no.89-3722) [17]. The crystallite size of the silver nanoparticles was calculated using the Debye-Scherer equation, and the average crystallite size was estimated to be 16nm. The X-ray diffraction studies confirmed the crystalline nature of silver nanoparticles.

Evaluation of Biological Applications of Silver Nanoparticles:

Antibacterial Activity of Silver nanoparticles: Out of three strains studied, antimicrobial profile was observed against *S. aureus* and *E. cloacae* with a clear zone of inhibition. However, no significant zone of inhibition was observed in agar plate swabbed with *E. coli* when treated with silver nanoparticles and thus stating the absence of anti-microbial activity. With an increase in the concentration of AgNPs an increased antibacterial action was observed **Fig. 6**.

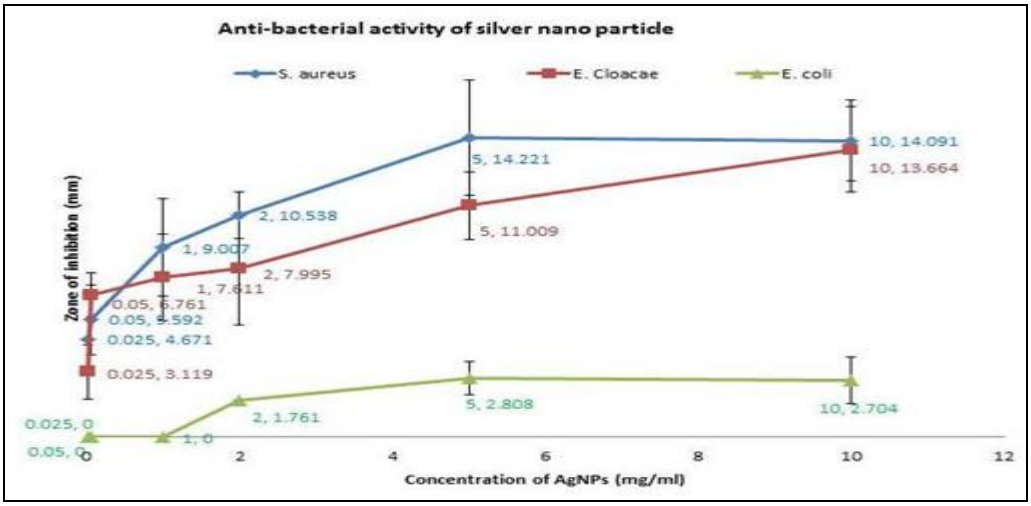

FIG. 6: ANTIBACTERIAL ACTIVITY OF SILVER NANOPARTICLES. All experiments were done in triplicate and the result expressed as average ± standard deviation.

Anti-Helminthic Activity of Silver Nanoparticles: The silver nanoparticles exhibited a concentration-dependent anti-helminthic activity. With the increase in the concentration of silver nanoparticles, the time taken for the paralysis and death of the helminths were significantly reduced **Fig. 7**. The study revealed that Albendazole, the positive control, was found to be less efficient than the silver nanoparticles **Table 3**.

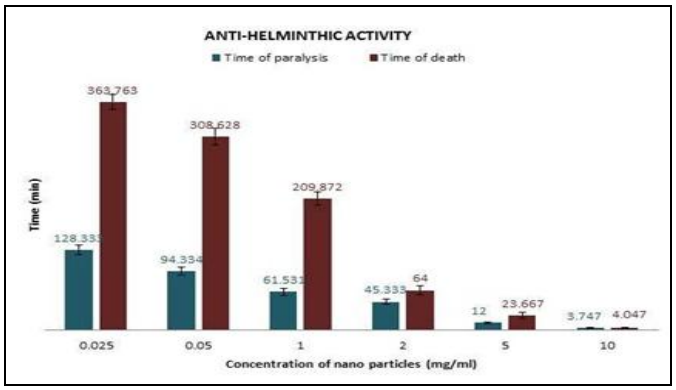

FIG. 7: ANTI-HELMINTHIC ACTIVITY OF SILVER NANOPARTICLES AGAINST *PHERETIMA POSTHUMA*

TABLE 3: COMPARATIVE EVALUATION OF ANTI-HELMINTHIC ACTIVITY

Samples at a concentration of 10 mg/ml	Paralysis time (min)	Death time (min)
Aq. extract of *S. androgynous*	11.009 ± 0.431	16. 873 ± 1.482
Silver nanoparticles	3.747 ± 0.287	4.047 ± 0.295
Albendazole	41.133 ± 1.073	51.836 ± 2. 642

The anti-helminthic effect of nanoparticles was revealed from the morphological changes, especially the loss of outer membrane from the body of the earthworm. This may indicate that the tegumental surface of earthworm, which was metabolically active, was severely damaged as evident from the loss of papillae, severe blebbing, shearing, and erosion of the surface structures. Such topographical disruptions would facilitate the penetration of the nanoparticles deep within the tissues that might greatly reduce the invasive potential of the helminth.

DISCUSSION: The free radical scavenging potential is attributed to the abundance of secondary metabolites and the high level of phenolic acid content in the plant. The conjugated aromatic ring structure, as well as hydroxyl and carbonyl groups in the phenolic compound, are reported to bind effectively to the metals, thereby inactivating ions through chelation. This is the widely accepted mechanism exhibited by phenolic compounds during free radicals and Reactive Oxygen Species quenching mechanism [18]. Hence, the estimated total phenolic content of *S. androgynous* contributes significantly towards its anti-oxidant potential **Table 2**.

The spectrum **Fig. 1** and **2** indicate that *S. androgynous* proves to be a good source for the synthesis of AgNPs, and this could be attributed to its anti-oxidant potential. Studies have reported that the anti-oxidant potential of plants is due to their redox properties, which allow them to act as reducing agents, hydrogen donators, metal chelators, and single oxygen quenchers [19]. Higher anti-oxidant potential means higher reducing components. The presence of these reducing agents is of great impact in green synthesis as they reduce metal ions into stable nanoparticles.

AgNPs have been reported to exhibit an absorption maximum around 420 nm due to their surface plasmon resonance. However, the range of peaks may extend from 400 nm to 500 nm depending on the size and shape of the nanoparticles synthesized. A number of factors like metal ion concentration, temperature, and incubation time determine the size and shape of the synthesized nanoparticles. In the present study, with an increase in the concentration of metal ions, the peak was found to be flattened and shifted to the visible range **Fig. 1**. The reports highlight that a shift of peak towards UV regions occurs as the particle size decreases and towards the visible region with an increase in sizes [20]. Hence, the flattened peaks obtained at higher concentrations of metal ions could possibly due to the synthesis of large-sized silver nanoparticles. Similarly, at a high temperature of 70 ºC, the characteristic sharp peak of silver nanoparticles was present, and no peaks were observed at lower temperatures **Fig. 2**. Earlier reports suggest that high temperature favors the formation of smaller silver nanoparticles by reducing the extent of aggregation of the nanoparticles due to an increase in the rate of adsorption of silver nitrate and the viscosity of the coating phase. The decrease in particle size with higher temperature may also be due to an increase in reaction rate, leading to the formation of nuclei from the silver ions and preventing the secondary reduction process on the surface of the pre-formed nuclei [21].

The possible mode of anti-microbial action of silver nanoparticles could be the disruption of membrane potential and integrity. Nanoparticles are reported to bind to the bacterial membranes via electrostatic interaction. It subsequently damages the membrane by altering its potential and then cross the bacterial membrane and gather along the metabolic pathway, influencing the shape and function of the cell membrane. Further, the Nano Particles interact with the bacterial cell's basic components, leading to oxidative stress and changes in cell membrane permeability and gene expression [5].

The role of secondary metabolites in anti-helminthic action is already reported. The suggested mechanism on the mortality of helminths is due to the binding of phytoconstituents with free proteins in the gastrointestinal tract or glycoprotein on the parasite cuticle [22]. In the present study, though the plant extract was found to be an effective anti-helminthic agent, the nanoparticles had a more pronounced effect, and it could be due to the synergistic effect of phytochemicals and capped phytoconstituents on silver nanoparticles. The result confirmed that the green synthesized silver nanoparticle could be effective against parasitic infection in humans.

CONCLUSION: In the present study, silver nanoparticles were synthesized using an aqueous extract of *S. androgynous*. The extract was found to be rich in secondary metabolites and phenolic compounds, thus significantly contributing to the process of green synthesis. Various parameters like metal ion concentration and incubation temperature for the synthesis were optimized. Characterization by UV-VIS spectrophotometry, FTIR, XRD, and SEM revealed characteristic features of silver nanoparticles. The biological properties were evaluated, and silver nanoparticles were found to

have effective antibacterial and anti-helminthic action.

ACKNOWLEDGEMENT: Authors acknowledge Marian Centre for Advanced Research (MCAR), St. Mary's College, Thrissur for providing the instrumentation facility, and Dr. Regi Raphael, Taxonomist and Head, Department of Botany, St. Mary's College, Thrissur, for identification of the plant sample.

CONFLICTS OF INTEREST: The authors declare that they have no known competing financial interests or personal relationships that could have appeared to influence the work reported in this paper.

REFERENCES:

1. Khan I, Saeed K and Khan I: Nanoparticles: Properties, applications and toxicities. Arabian Journal of Chemistry 2019; 12: 908-31.
2. Iravani S, Korbekandi H, Mirmohammadi SV and Zolfaghari B: Synthesis of silver nanoparticles: chemical, physical and biological methods. Research in Pharmaceutical Sciences 2014; 9(6): 385-406.
3. Khan I, Saeed K and Khan I: Nanoparticles: Properties, applications and toxicities. Arabian Journal of Chemistry 2019; 12(7): 908-31.
4. Rizwan M, Singh M, Mitra CK and Morve RK: Ecofriendly Application of Nanomaterials: Nano-bioremediation. Journal of Nanoparticles 2014; 1-7.
5. Wang L, Hu C and Shao L: The antimicrobial activity of nanoparticles: present situation and prospects for the future. International Journal of Nanomedicine 2017; 12: 1227-49.
6. Aderibigbe BA: Metal-based nanoparticles for the treatment of infectious diseases. Molecules 2017; 22: 1-37.
7. Niknejad F, Nabili M, Ghazvini DR and Moazeni M: Green synthesis of silver nanoparticles: Advantages of the yeast Saccharomyces cerevisiae model. Current Medical Mycology 2015; 1(3): 17-24.
8. Mandava K: Biological and Non-biological Synthesis of Metallic Nanoparticles: Scope for Current Pharmaceutical Research. Indian J Pharm Sci 2017; 79(4): 501-12.
9. Singh J, Dutta T, Kim KH, Rawat M, Samddar P and Kumar P: Green synthesis of metals and their oxide nanoparticles: applications for environmental remediation. Journal of Nanobiotechnology 2018; 16(1): 1-24.
10. Kalpana VN and Rajeswari VD: A review on green synthesis, biomedical applications, and toxicity studies of ZnO NPs. Bioinorganic Chemistry and Applications 2018; 74(2): 1-12.
11. Ahmad S, Munir S, Zeb N and Ullah A: Green nanotechnology: a review on green synthesis of silver nanoparticles - an ecofriendly approach. International Journal of Nanomedicine 2019; 14: 5087-5107.
12. Zenebe S, Feyera T and Assefa S: *In-vitro* anthelmintic activity of crude extracts of aerial parts of *Cissus quadrangularis* L. and leaves of *Schinus molle* L. against *Haemonchus contortus*. BioMed Research International 2017; 16: 1-6.
13. Sasidharan S, Chen Y, Saravanan D, Sundram KM and Yoga Latha L: Extraction, isolation and characterization of bioactive compounds from plants' extracts. African Journal of Traditional, Complementary, and Alternative Medicines 2011; 8(1): 1-10.
14. Stankovic MS: Total phenolic content, flavonoid concentration and antioxidant activity of *Marrubium peregrinum* L. extracts. Kragujevac J Sci 2011; 33: 63-72.
15. Kumar B, Smita K, Vizuete KS and Kumar LC: Aqueous phase lavender leaf mediated green synthesis of gold nanoparticles and evaluation of its antioxidant activity. Biol Med 2016; 8(3): 1-4.
16. Soman S and Ray JG: Silver nanoparticles synthesized using aqueous leaf extract of *Ziziphus oenoplia* (L.) Mill: Characterization and assessment of antibacterial activity. Journal of Photochemistry and Photobiology B: Biology 2016; 163: 391-402.
17. Anandalakshmi K, Venugobal J and Ramasamy V: Characterization of silver nanoparticles by green synthesis method using *Pedalium murex* leaf extract and their antibacterial activity. Applied Nanoscience 2016; 6: 399-408.
18. Lin J, Liu S, Kuo L and Yang D: Composition of phenolic compounds and antioxidant attributes of *Cyclea gracillima* Diels extracts. Journal of Food and Drug Analysis 2018; 26: 193-200.
19. Gulcin I: Antioxidants and antioxidant methods: an updated overview. Archives of Toxicology 2020; 94: 651–715.
20. Kuiri PK: Control of ultraviolet surface plasmon absorption of al nanoparticles by changing particle size, shape, interaction, and medium dielectric constant. Plasmonics 2020; 15: 933-40.
21. Gurunathan S, Kalishwaralal K, Vaidyanathan R, Deepak V and Pandian SRK: Biosynthesis, purification and characterization of silver nanoparticles using Escherichia coli. Colloid Surf B 2009; 74: 328-35.
22. Rashid MM, Ferdous J, Banik S and Islam MR: Anthelmintic activity of silver-extract nanoparticles synthesized from the combination of silver nanoparticles and *M. charantia* fruit extract. BMC Complementary and Alternative Medicine 2016; 16(242): 1-6.

How to cite this article:
Abhimannue AP and Menon A: Green synthesis of silver nanoparticles using *Sauropus androgynous* leaf extract with potential biological properties. Int J Pharm Sci & Res 2021; 12(8): 4267-74. doi: 10.13040/IJPSR.0975-8232.12(8).4267-74.